

Theoretical and Experimental Characterization of Pyrazolato-Based Ni(II) Metal Organic Frameworks

Elisa Albanese,[†] Bartolomeo Civalleri,^{*,†} Matteo Ferrabone,[†] Francesca Bonino,[†]
Simona Galli,[‡] Angelo Maspero,[‡] and Claudio Pettinari[¶]

*Dipartimento di Chimica IFM e Centro di Eccellenza NIS, Università di Torino, Via P. Giuria 7
10125 Torino (Italy), Dipartimento di Scienza e Alta Tecnologia, Università dell'Insubria, Via
Valleggio 11, I-22100 Como, Italy, and Scuola di Scienze del Farmaco e dei Prodotti della Salute,
Università di Camerino, Via S. Agostino 1, I-62032 Camerino (MC), Italy*

E-mail: bartolomeo.civalleri@unito.it

*To whom correspondence should be addressed

[†]Università di Torino

[‡]Università dell'Insubria

[¶]Università di Camerino

Stability of magnetic phases

The relative stability of Ni-bpz and Ni-bpb with Ni(II) in both low spin (LS) and high spin (HS) configuration, within diamagnetic (DIA), antiferromagnetic (AFM) and ferromagnetic (FM) unit cells, has been studied on the experimental structures. To investigate all possible magnetic phases (i.e. DIA-LS, AFM-HS and FM-HS) the primitive unit cell, derived from the experimentally determined one in *Imma*, and containing two symmetry-related Ni atoms, has been modified by lowering the symmetry to the monoclinic space group *I12/m1*. In this way, the unit cell contains now two independent metal ions which can have opposite HS state (i.e. Ni₁(↑↑) and Ni₂(↓↓)) and the AFM-HS phase can be built. For sake of consistency, we used this crystallographic symmetry to compute the relative stability of all the different magnetic phases, even if the original space group can be used for the DIA-LS and FM-HS phases. Results reported in Table S1 show that the diamagnetic phase is the most stable one with a remarkable energy difference with respect to the other two phases. This is not unexpected because it is well known that Ni(II) in square planar coordination prefers a low spin state.

Table S1: Relative stability of Ni-bpz and Ni-bpb with Ni(II) in both low spin (LS) and high spin (HS) configuration in kJ/mol per Ni atom.

	DIA-LS	AFM-HS	FM-HS
Ni-bpz	0.0	63.9	64.8
Ni-bpb	0.0	65.0	71.0

Activation of the samples

Ni-bpz

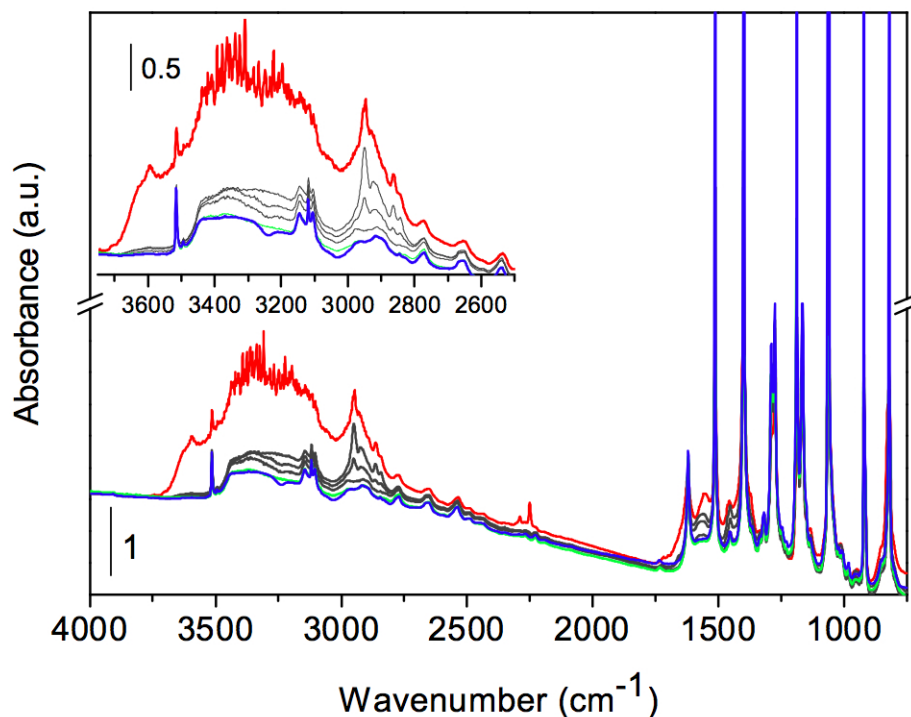


Figure S1: FTIR spectra of Ni-bpz as such (red curve), outgassed at RT, 80 °C, 120 °C (gray curves), 150 °C for 2 h (green curve) and 150 °C for one night (blue curve). The inset reports the 3750 - 2500 cm⁻¹ range.

FTIR spectra were acquired on Ni-bpz as such and after thermal treatment at different temperatures under high vacuum (Figure S1). The persistence of the band centered at 3500 cm⁻¹ in all the acquired spectra, suggests that some solvent remains trapped even after prolonged evacuation under high vacuum.

Ni-bpb

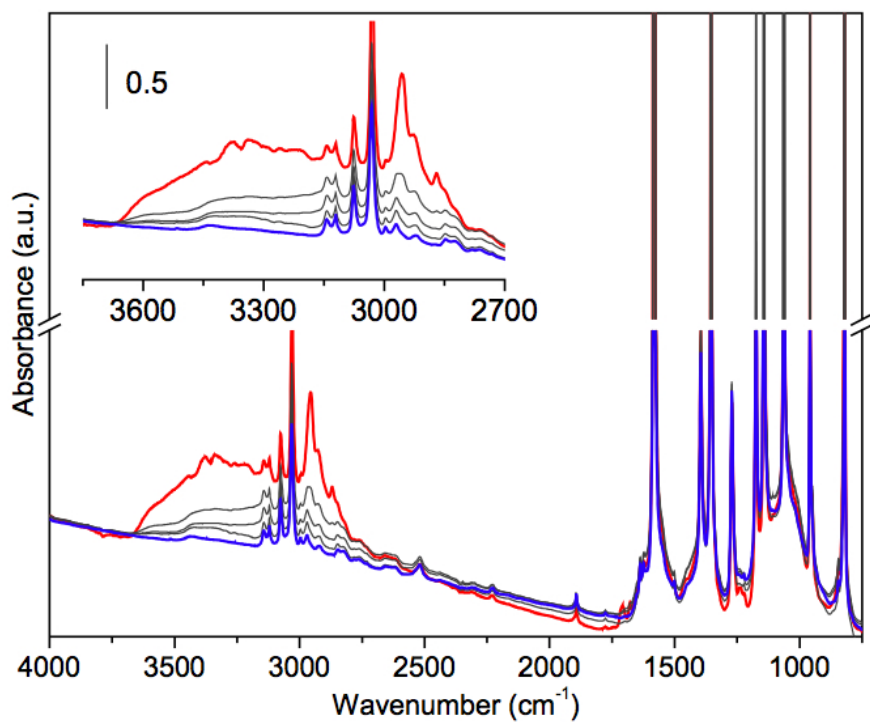


Figure S2: FTIR spectra of Ni-bpb as such (red curve), outgassed at RT, 80 °C, 120 °C (gray curves), and at 180 °C for 2 h (blue curve). The inset reports the 3750 - 2700 cm⁻¹ range.

FTIR spectra were acquired on Ni-bpb as such and after thermal treatment at different temperatures under high vacuum (Figure S2). In this case, upon thermal treatment, the band centered at 2900 cm⁻¹ is progressively eroded, witnessing that the clathrated solvent can be easily removed.

Adsorption of CO₂ on Ni-bpb

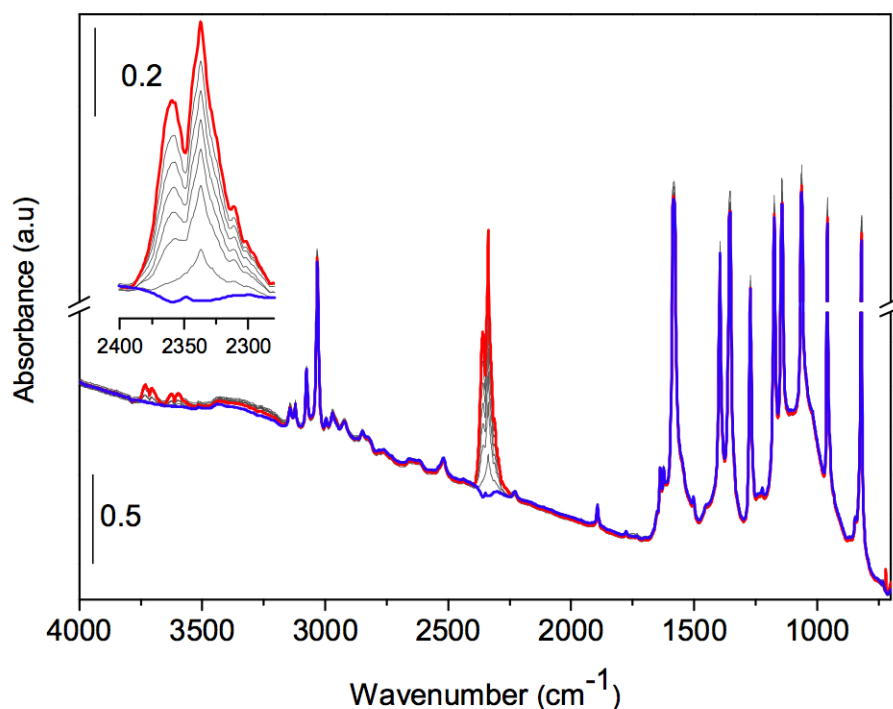


Figure S3: FTIR spectra of CO₂ adsorbed at RT on Ni-bpb. The blue curve is the spectrum of the sample activated at 180 °C for 2 h, while the red curve represents the maximum coverage of CO₂. In the inset, the CO₂ asymmetric stretching region is magnified.

At low coverage a band at 2338 cm⁻¹ is clearly present and it can be ascribed to CO₂ adsorbed inside the cavities, acting as electron acceptor, e.g. towards the organic linkers. At increasing coverage, a band at 2358 cm⁻¹ appears, suggesting that CO₂ is going towards the liquid-like form. By considering these experimental evidences, the interaction between CO₂ and Ni(II) sites can not be hypothesized.^{1,2} In the high frequency region (3800-3500 cm⁻¹), two components are observed at 3666 and 3580 cm⁻¹. The nature of these two absorptions is well known and is interpreted on the basis of the combination of ν_1 and ν_3 modes of CO₂. The reason for the presence of a doublet shifted by about ± 50 cm⁻¹ from the expected frequency for the combination mode ν_1 and ν_3 , is due to the fact that the first overtone of the ν_2 mode coincides with the ν_1 mode, causing a strong Fermi resonance effect that induces a band splitting in two components 100 cm⁻¹ apart.^{3,4}

Adsorption of CO on Ni-bpb

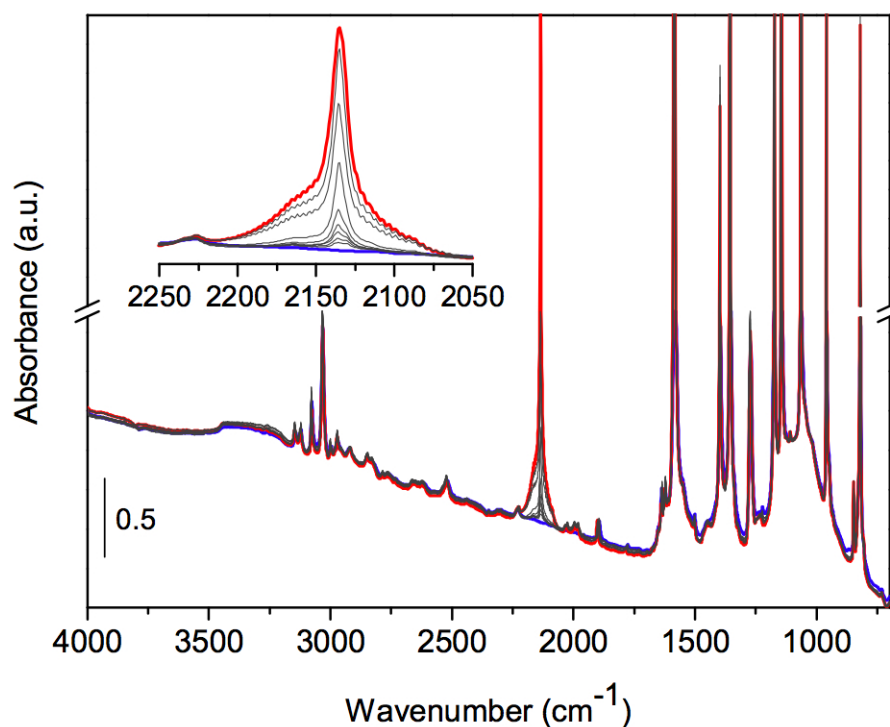


Figure S4: FTIR spectra of CO adsorbed on Ni-bpb at 77 K. The blue curve is the spectrum of the sample activated at 180 °C for 2 h, while the red curve represents the maximum coverage of CO. In the inset, the CO asymmetric stretching region is magnified.

The $\nu(CO)$ frequency is quite near that of the unperturbed molecule (2143 cm^{-1} , gas phase); at variance, in the presence of interactions with Ni(II) open sites, a non negligible shift was observed (for instance, the band lies at 2178 cm^{-1} in the case of activated CPO-27-Ni).⁵

Vibrational Frequencies: Calculated and Experimental spectra in the C-H stretching region

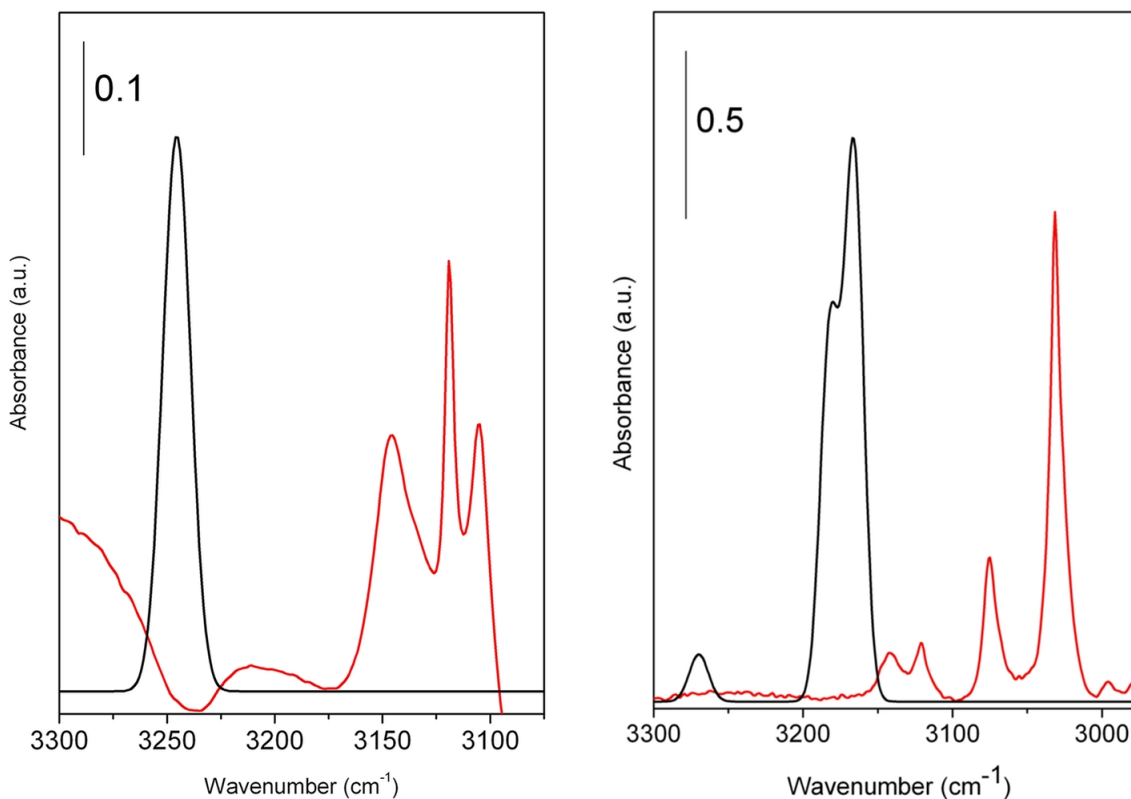


Figure S5: CH stretching region of calculated (black) and experimental (red) spectra of Ni-bpz (left) and Ni-bpb (right). The simulated spectra have been computed by using a Lorentzian function with a FWHM of 15 cm^{-1} .

In this range the agreement between calculated and experimental spectra is less satisfactory in comparison with the lower frequency range.

Rietveld refinement of Ni-bpz

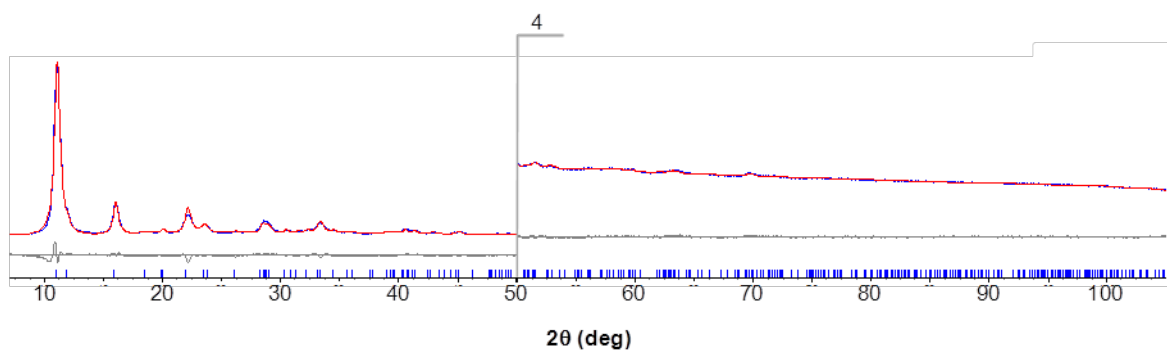


Figure S6: Graphical results of the Rietveld refinement carried out on Ni-bpz at 130 °C, in terms of experimental, calculated and difference traces (blue, red and gray, respectively). The markers of the Bragg peaks are reported at the bottom. Horizontal axis, 2θ (deg); vertical axis, intensity (counts). The portion above 50 deg has been magnified for the sake of clarity.

CRYSTAL input file

Ni-bpz optimized diamagnetic structure

Ni-bpz optimized diamagnetic structure

CRYSTAL

1 0 0

I M M A

14.59673226 7.02656184 10.14232169

28	0.000000000000E+00	1.239501767924E-19	0.000000000000E+00
28	0.000000000000E+00	-5.000000000000E-01	0.000000000000E+00
6	-2.097479067840E-01	-2.500000000000E-01	2.074973324479E-01
6	2.097479067840E-01	-2.500000000000E-01	2.074973324479E-01
6	-2.097479067840E-01	2.500000000000E-01	-2.074973324479E-01
6	2.097479067840E-01	2.500000000000E-01	-2.074973324479E-01
6	-1.621297946118E-01	-9.388257328239E-02	1.561686395962E-01
6	1.621297946118E-01	-4.061174267176E-01	1.561686395962E-01
6	-1.621297946118E-01	9.388257328239E-02	-1.561686395962E-01
6	1.621297946118E-01	4.061174267176E-01	-1.561686395962E-01
6	1.621297946118E-01	9.388257328239E-02	-1.561686395962E-01
6	-1.621297946118E-01	4.061174267176E-01	-1.561686395962E-01
6	1.621297946118E-01	-9.388257328239E-02	1.561686395962E-01
6	-1.621297946118E-01	-4.061174267176E-01	1.561686395962E-01
1	-1.751496918073E-01	5.619545841890E-02	1.675261293924E-01
1	1.751496918073E-01	4.438045415811E-01	1.675261293924E-01
1	-1.751496918073E-01	-5.619545841890E-02	-1.675261293924E-01
1	1.751496918073E-01	-4.438045415811E-01	-1.675261293924E-01
1	1.751496918073E-01	-5.619545841890E-02	-1.675261293924E-01
1	-1.751496918073E-01	-4.438045415811E-01	-1.675261293924E-01
1	1.751496918073E-01	5.619545841890E-02	1.675261293924E-01
1	-1.751496918073E-01	4.438045415811E-01	1.675261293924E-01
7	-9.186691398146E-02	-1.537975605022E-01	8.134652403069E-02
7	9.186691398146E-02	-3.462024394978E-01	8.134652403069E-02

```
7 -9.186691398146E-02 1.537975605022E-01 -8.134652403069E-02
7 9.186691398146E-02 3.462024394978E-01 -8.134652403069E-02
7 9.186691398146E-02 1.537975605022E-01 -8.134652403069E-02
7 -9.186691398146E-02 3.462024394978E-01 -8.134652403069E-02
7 9.186691398146E-02 -1.537975605022E-01 8.134652403069E-02
7 -9.186691398146E-02 -3.462024394978E-01 8.134652403069E-02
```

OPTGEOM

FULLOPTG

ALLOWTRISTR

BFGS

MAXCYCLE

150

FINALRUN

4

ENDOPT

ENDG

6 5

0 0 6 2.0 1.00

0.4563240000D+04 0.1966650000D-02

0.6820240000D+03 0.1523060000D-01

0.1549730000D+03 0.7612690000D-01

0.4445530000D+02 0.2608010000D+00

0.1302900000D+02 0.6164620000D+00

0.1827730000D+01 0.2210060000D+00

0 1 3 4.0 1.00

0.2096420000D+02 0.1146600000D+00 0.4024870000D-01

0.4803310000D+01 0.9199990000D+00 0.2375940000D+00

0.1459330000D+01 -0.3030680000D-02 0.8158540000D+00

0 1 1 0.0 1.00

0.4834560000D+00 0.1000000000D+01 0.1000000000D+01

0 1 1 0.0 1.00

0.1455850000D+00 0.1000000000D+01 0.1000000000D+01

0 3 1 0.0 1.00

0.6260000000D+00 0.1000000000D+01
7 5
0 0 6 2.0 1.00
0.6293480000D+04 0.1969790000D-02
0.9490440000D+03 0.1496130000D-01
0.2187760000D+03 0.7350060000D-01
0.6369160000D+02 0.2489370000D+00
0.1882820000D+02 0.6024600000D+00
0.2720230000D+01 0.2562020000D+00
0 1 3 5.0 1.00
0.3063310000D+02 0.1119060000D+00 0.3831190000D-01
0.7026140000D+01 0.9216660000D+00 0.2374030000D+00
0.2112050000D+01 -0.2569190000D-02 0.8175920000D+00
0 1 1 0.0 1.00
0.6840090000D+00 0.1000000000D+01 0.1000000000D+01
0 1 1 0.0 1.00
0.2008780000D+00 0.1000000000D+01 0.1000000000D+01
0 3 1 0.0 1.00
0.9130000000D+00 0.1000000000D+01
1 4
0 0 3 1.0 1.00
0.3386500000D+02 0.2549380000D-01
0.5094790000D+01 0.1903730000D+00
0.1158790000D+01 0.8521610000D+00
0 0 1 0.0 1.00
0.3258400000D+00 0.1000000000D+01
0 0 1 0.0 1.00
0.1027410000D+00 0.1000000000D+01
0 2 1 0.0 1.00
0.7500000000D+00 0.1000000000D+01
28 11
0 0 8 2.0 1.0
351535.72935 .22529386884E-03

52695.809283	.17468616223E-02
11992.468293	.90849992136E-02
3394.5776689	.36940748447E-01
1105.3594585	.12032819950
397.14677769	.28596715057
154.27542974	.40983020196
61.018723780	.21620642851
0 0 4 2.0 1.0	
384.45559739	-.24651279268E-01
119.04879199	-.11658505277
19.137012223	.54864126676
8.1526718562	.52640051122
0 0 2 2.0 1.0	
12.579408642	-.22797884293
2.0870866081	.70703738215
0 0 1 2.0 1.0	
.86432568555	1.0000000000
0 0 1 0.0 1.0	
.13283169217	1.0000000000
0 2 6 6. 1.00	
1883.0907486	.23748258443E-02
445.95155320	.19289457172E-01
143.08430815	.90718211507E-01
53.372920722	.26181414117
21.321919357	.42309149832
8.6643561994	.24641686015
0 2 3 6. 1.00	
34.144255211	-.29677129163E-01
4.7122455921	.55616824096
1.8709231845	.96357766460
0 2 1 0. 1.00	
.70370016267	1.0000000000
0 3 4 8. 1.00	

```
74.591603465      .12077454672E-01
21.590632752      .74637262154E-01
7.6246142580      .23236775502
2.8632206762      .39042651680
0 3 1 0. 1.00
1.0311063388      .39509498921
0 3 1 0. 1.00
.33060760691      .21138769167
99 0
ENDB
DFT
B3LYP
SPIN
XLGRID
END
SCFDIR
FDOCCUP
2
1 9 3
1 1 1 0 1
1 1 1 0 1
2 9 3
1 1 1 0 1
1 1 1 0 1
EIGSHIFT
2
1 9 4 3. 3.
2 9 4 3. 3.
SPINLOCK
0 100
SHRINK
3 6
TOLINTEG
```

7 7 7 7 20

FMIXING

90

BROYDEN

0.05 50 10

TOLDEE

7

MAXCYCLE

100

ENDSCF

Ni-bpb optimized diamagnetic structure

Ni-bpb

CRYSTAL

1 0 0

I 1 1 2/B

	7.01154566	21.72814300	15.05238158	89.755915
28	2.500000000000000E-01	2.500000000000000E-01	2.500000000000000E-01	
6	3.425822634715E-01	-1.416453322773E-01	-1.428857004343E-01	
6	3.445829830157E-01	1.398510359295E-01	1.475311277319E-01	
6	1.554170169843E-01	-1.398510359295E-01	-3.524688722681E-01	
6	-3.445829830157E-01	-1.398510359295E-01	-1.475311277319E-01	
6	-1.554170169843E-01	1.398510359295E-01	3.524688722681E-01	
6	4.991683716742E-01	-1.084665879312E-01	-1.111733127195E-01	
6	8.316283258319E-04	1.084665879312E-01	3.888266872805E-01	
6	-4.991683716742E-01	1.084665879312E-01	1.111733127195E-01	
6	-8.316283258319E-04	-1.084665879312E-01	-3.888266872805E-01	
6	4.995264626423E-01	-5.339366938276E-02	-5.458427900174E-02	
6	4.735373576861E-04	5.339366938276E-02	4.454157209983E-01	
6	-4.995264626423E-01	5.339366938276E-02	5.458427900174E-02	
6	-4.735373576861E-04	-5.339366938276E-02	-4.454157209983E-01	

6 3.553207317566E-01 -4.292341852398E-02 8.300790442108E-03
6 1.446792682434E-01 4.292341852398E-02 -4.916992095579E-01
6 -3.553207317566E-01 4.292341852398E-02 -8.300790442108E-03
6 -1.446792682434E-01 -4.292341852398E-02 4.916992095579E-01
6 3.557748322017E-01 9.256014210160E-03 6.161908279410E-02
6 1.442251677983E-01 -9.256014210160E-03 -4.383809172059E-01
6 -3.557748322017E-01 -9.256014210160E-03 -6.161908279410E-02
6 -1.442251677983E-01 9.256014210160E-03 4.383809172059E-01
7 4.023499802989E-01 -1.887702791312E-01 -1.935281380290E-01
7 9.765001970115E-02 1.887702791312E-01 3.064718619710E-01
7 -4.023499802989E-01 1.887702791312E-01 1.935281380290E-01
7 -9.765001970115E-02 -1.887702791312E-01 -3.064718619710E-01
7 4.046630386191E-01 1.877722025153E-01 1.962165056542E-01
7 9.533696138085E-02 -1.877722025153E-01 -3.037834943458E-01
7 -4.046630386191E-01 -1.877722025153E-01 -1.962165056542E-01
7 -9.533696138085E-02 1.877722025153E-01 3.037834943458E-01
1 2.436636386510E-01 -7.677956293884E-02 1.708384508742E-02
1 2.563363613490E-01 7.677956293884E-02 -4.829161549126E-01
1 -2.436636386510E-01 7.677956293884E-02 -1.708384508742E-02
1 -2.563363613490E-01 -7.677956293884E-02 4.829161549126E-01
1 2.445967643984E-01 1.510645197213E-02 1.110381951199E-01
1 2.554032356016E-01 -1.510645197213E-02 -3.889618048801E-01
1 -2.445967643984E-01 -1.510645197213E-02 -1.110381951199E-01
1 -2.554032356016E-01 1.510645197213E-02 3.889618048801E-01
1 1.923242210646E-01 -1.330065220170E-01 -1.339716217060E-01
1 3.076757789354E-01 1.330065220170E-01 3.660283782940E-01
1 -1.923242210646E-01 1.330065220170E-01 1.339716217060E-01
1 -3.076757789354E-01 -1.330065220170E-01 -3.660283782940E-01
1 1.943601962782E-01 1.306319342895E-01 1.408829068832E-01
1 3.056398037218E-01 -1.306319342895E-01 -3.591170931168E-01
1 -1.943601962782E-01 -1.306319342895E-01 -1.408829068832E-01
1 -3.056398037218E-01 1.306319342895E-01 3.591170931168E-01

END

Atomic basis sets reported above

ENDB

DFT

B3LYP

SPIN

XLGRID

END

SCFDIR

FDOCCUP

2

1 9 3

1 1 1 0 1

1 1 1 0 1

2 9 3

1 1 1 0 1

1 1 1 0 1

EIGSHIFT

2

1 9 4 3. 3.

2 9 4 3. 3.

SPINLOCK

0 100

SHRINK

3 6

TOLINTEG

7 7 7 7 20

FMIXING

90

BROYDEN

0.05 50 10

TOLDEE

7

MAXCYCLE

100

ENDSCF

Calculated IR and Raman Vibrational Frequencies

Table S2: Calculated IR vibrational frequencies of Ni-bpz. The frequencies (cm^{-1}), the symmetry and the intensities of all the modes are reported.

MODES	FREQUENCIES (cm^{-1})	IRREP	INTENS (Km/mol)
1	60.01570	B3U	1.04
4	107.8431	B1U	0.13
6	114.7454	B2U	0.46
9	194.6319	B3U	2.80
12	273.2512	B1U	1.21
13	274.2583	B2U	3.17
15	314.6574	B3U	25.43
17	337.4501	B1U	1.35
21	409.9358	B1U	53.35
22	460.4942	B3U	86.53
23	460.5192	B2U	62.69
28	648.5929	B1U	61.29
29	651.8949	B2U	24.52
33	679.2741	B3U	16.90
36	811.4925	B3U	0.11
40	848.2963	B1U	92.53
41	849.9539	B2U	54.99
44	939.0057	B2U	69.00
45	939.1889	B1U	66.68
50	1049.9206	B3U	0.09
52	1080.0807	B1U	171.61
53	1083.2422	B2U	183.17
57	1187.6487	B3U	170.65
60	1211.1854	B2U	153.22
61	1214.0882	B1U	65.15
64	1315.0025	B1U	167.87
65	1316.7695	B2U	178.54

Table S2: continued on the next page

Table S2: continued from previous page

MODES	FREQUENCIES (cm ⁻¹)	IRREP	INTENS (km/mol)
66	1354.5769	B3U	0.77
73	1428.9938	B3U	233.92
76	1549.1627	B2U	112.71
77	1552.6872	B1U	44.84
82	3245.1195	B2U	12.47
83	3245.3567	B1U	1.78
85	3246.7698	B3U	5.23

Table S3: Calculated Raman vibrational frequencies of Ni-bpz. The frequencies (cm^{-1}), the symmetry of all the modes are reported.

MODES	FREQUENCIES (cm^{-1})	IRREP
3	71.7242	B1G
5	109.6625	B3G
7	136.729	B2G
10	222.0978	AG
11	232.1246	B1G
14	299.2818	B2G
18	385.3912	B3G
20	408.0635	AG
24	482.2313	B1G
25	489.9981	B3G
26	490.5388	B2G
27	511.8245	AG
30	661.3586	B1G
32	672.8255	B3G
34	679.3964	AG
35	685.759	B2G
38	820.4835	B1G
39	825.7421	B2G
42	863.6003	B3G
43	864.9438	AG
46	1029.0724	B1G
47	1040.6567	B3G
48	1041.3057	AG
49	1047.1837	B2G
54	1116.3995	B3G
55	1131.6351	AG
56	1181.5382	B1G
59	1198.0351	B2G

Table S3: continued on the next page

Table S3: continued from previous page

MODES	FREQUENCIES (cm ⁻¹)	IRREP
62	1289.1081	B3G
63	1298.6606	AG
68	1406.6252	B1G
69	1411.8753	B3G
70	1413.1299	B2G
71	1415.5902	AG
74	1453.2998	B1G
75	1456.0565	B2G
78	1650.9154	AG
79	1651.4621	B3G
80	3242.8291	B2G
81	3243.0986	B1G
86	3249.5211	AG
87	3249.595	B3G

Table S4: Calculated IR vibrational frequencies of Ni-bpb. The frequencies (cm^{-1}), the symmetry and the intensities of all the modes are reported.

MODES	FREQUENCIES (cm^{-1})	IRREP	INTENS (Km/mol)
3	44.7048	AU	0.01
4	47.3618	BU	0.05
5	59.1408	AU	0.14
6	61.5050	BU	0.78
10	141.3970	AU	0.87
12	148.1274	BU	3.53
16	199.8342	AU	1.67
17	213.9573	BU	0.42
18	250.5356	BU	0.73
21	275.3000	BU	6.07
22	280.4401	AU	1.21
23	316.0732	AU	0.49
25	329.3557	BU	5.87
26	337.4902	AU	3.63
28	377.8037	BU	21.66
30	388.2055	AU	4.62
31	414.2712	BU	1.61
32	414.6686	AU	0.61
33	416.5465	BU	44.28
36	461.6743	AU	1.31
37	474.3071	BU	44.15
40	530.2420	BU	54.16
41	546.2136	AU	49.42
42	552.0761	BU	63.24
43	554.7470	AU	55.45
47	666.2480	BU	45.25
48	669.3019	AU	16.33
49	673.0671	AU	7.99

Table S4: continued on the next page

Table S4: continued from previous page

MODES	FREQUENCIES (cm ⁻¹)	IRREP	INTENS (Km/mol)
53	685.7302	BU	16.35
59	830.2833	BU	7.96
61	833.6930	AU	1.91
62	841.2412	BU	160.08
63	843.6989	AU	66.63
68	874.5516	AU	8.25
69	875.0986	BU	25.15
72	970.2781	BU	12.45
73	971.5593	AU	17.49
75	976.6130	AU	81.07
76	976.7713	BU	76.08
79	1034.5324	AU	0.43
80	1034.7296	BU	0.96
81	1044.2836	BU	0.10
82	1044.5178	AU	0.14
86	1081.8894	BU	148.97
87	1083.7018	AU	166.88
88	1134.7017	BU	1.21
89	1135.4830	AU	1.50
92	1164.9498	AU	212.34
93	1165.7795	BU	95.37
95	1192.9393	BU	181.93
97	1197.0754	AU	0.00
102	1292.0562	BU	0.37
103	1292.3193	AU	1.51
104	1296.6566	AU	49.51
105	1297.6317	BU	74.39
108	1382.1942	AU	226.01
109	1382.7273	BU	150.11
110	1387.7142	BU	27.55

Table S4: continued on the next page

Table S4: continued from previous page

MODES	FREQUENCIES (cm ⁻¹)	IRREP	INTENS (Km/mol)
111	1388.2597	AU	0.00
117	1421.2704	AU	0.16
119	1425.9179	BU	195.67
120	1464.4413	BU	0.72
121	1464.8733	AU	0.23
122	1533.0684	AU	0.02
123	1533.8057	BU	1.55
128	1605.7580	AU	358.26
129	1607.7845	BU	157.15
132	3164.6780	BU	46.65
133	3164.7769	AU	44.78
136	3182.5843	BU	52.02
137	3182.6648	AU	16.23
140	3248.1748	AU	2.08
142	3248.3639	BU	0.99
144	3268.8752	AU	3.87
145	3269.0876	BU	0.73

Table S5: Calculated Raman vibrational frequencies of Ni-bpb. The frequencies (cm^{-1}) and the symmetry of all the modes are reported.

MODES	FREQUENCIES (cm^{-1})	IRREP
1	32.2789	BG
2	41.9432	AG
7	61.6959	BG
8	88.8125	BG
9	120.1260	AG
11	144.0327	AG
13	162.1580	BG
14	181.1884	AG
15	192.3691	BG
19	263.7947	AG
20	267.4030	BG
24	323.1037	AG
27	361.0053	BG
29	382.4543	AG
34	419.1165	BG
35	434.0219	AG
38	490.6327	BG
39	495.2785	AG
44	646.8404	BG
45	649.3593	AG
46	660.0054	BG
50	673.3221	BG
51	678.7893	AG
52	684.1637	AG
54	739.1414	BG
55	740.9025	AG
56	750.5837	BG
57	751.0720	AG

Table S5: continued on the next page

Table S5: continued from previous page

MODES	FREQUENCIES (cm ⁻¹)	IRREP
58	828.7679	BG
60	832.8917	AG
64	846.0695	BG
65	848.0289	AG
66	865.7949	BG
67	869.0150	AG
70	963.3136	BG
71	964.7188	AG
74	976.3002	BG
77	977.5560	AG
78	1031.8622	BG
83	1049.7471	AG
84	1073.6992	BG
85	1080.7324	AG
90	1145.1431	BG
91	1155.6678	AG
94	1182.5447	BG
96	1197.0643	AG
98	1213.1051	BG
99	1213.8966	AG
100	1282.2984	BG
101	1291.8637	AG
106	1323.1005	BG
107	1323.8127	AG
112	1391.2444	BG
113	1394.6373	AG
114	1404.0614	BG
115	1407.1090	AG
116	1415.7530	BG
118	1422.4206	AG

Table S5: continued on the next page

Table S5: continued from previous page

MODES	FREQUENCIES (cm ⁻¹)	IRREP
124	1588.5592	AG
125	1588.9497	BG
126	1594.4426	BG
127	1594.6942	AG
130	1657.1169	BG
131	1658.3186	AG
134	3165.2250	BG
135	3165.2965	AG
138	3185.5320	BG
139	3185.6216	AG
141	3248.3199	AG
143	3248.4341	BG
146	3269.0897	AG
147	3269.1590	BG

References

- (1) Dietzel, P. D. C.; Johnsen, R. E.; Fjellvå, H.; Bordiga, S.; Groppo, E.; Chavan, S.; Blom, R. *Chem. Commun.* **2008**, *41*, 5125–5127.
- (2) Kandiah, M.; Nilsen, M. H.; Usseglio, S.; Jakobsen, S.; Olsbye, U.; Tilset, M.; Larabi, C.; Quadrelli, E. A.; Bonino, F.; Lillerud, K. P. *Chem. Mater.* **2010**, *22*, 6632–6640.
- (3) Bordiga, S.; Regli, L.; Bonino, F.; Groppo, E.; Lamberti, C.; Xiao, B.; Wheatley, P. S.; Morris, R. E.; Zecchina, A. *Phys. Chem. Chem. Phys.* **2007**, *9*, 2676.
- (4) Usseglio, S.; Damin, A.; Scarano, D.; Bordiga, S.; Zecchina, A.; Lamberti, C. *J. Am. Chem. Soc.* **2007**, *129*, 2822.
- (5) Chavan, S.; Bonino, F.; Vitillo, J. G.; Groppo, E.; Lamberti, C.; Dietzel, P. D. C.; Zecchina, A.; Bordiga, S. *Phys. Chem. Chem. Phys.* **2009**, *11*, 9811–9822.